Combinatorial catalyst development methods

T. E. Mallouk and E. S. Smotkin

Volume 2, Part 3, pp 334–347

in

Handbook of Fuel Cells – Fundamentals, Technology and Applications
(ISBN: 0-471-49926-9)

Edited by

Wolf Vielstich
Arnold Lamm
Hubert A. Gasteiger

© John Wiley & Sons, Ltd, Chichester, 2003

Chapter 23
Combinatorial catalyst development methods

T. E. Mallouk[1] and E. S. Smotkin[2]

[1] *Pennsylvania State University, University Park, PA, USA*
[2] *Illinois Institute of Technology, Chicago, IL, USA*

1 INTRODUCTION

1.1 Combinatorial materials chemistry

Combinatorial chemistry can be described as a systematic, Edisonian approach to the discovery of molecules and materials with enhanced properties. Unlike Edison's famous empirical search for a durable light bulb filament, the modern combinatorial method leverages parallel synthesis and screening in order to reduce the time and expense of discovery and optimization. While combinatorial chemistry has been very widely applied to biomolecular problems – in particular to drug discovery – over the last two decades, the method was in fact originally developed for research in catalysis. Over 90 years ago, Mittasch assembled arrays of reactors to discover better catalysts for ammonia synthesis.[1] He tested thousands of combinations of catalysts, supports, and promoters in a systematic manner, contributing substantially to the genesis of the Haber–Bosch process.

Several decades later, the combinatorial method was applied to other inorganic materials problems. Hanak used a continuous phase-spread approach to optimize the composition of alloy superconductors,[2] and Schultz, Xiang, and co-workers made discrete composition libraries for the discovery of high-T_c superconductors and magnetoresistive oxides.[3] These more modern examples of the combinatorial method used planar arrays of microscale samples, permitting more rapid searches through large numbers of compositions. Related high-throughput methods have been used over the past several years to accelerate the search for numerous classes of inorganic materials, including superconductors,[2, 3] phosphors,[4] dielectrics,[5] and sensor materials.[6]

1.2 Combinatorial methods for the discovery of heterogeneous catalysts

While catalysis is a science, it is an imprecise one. A catalytic reaction can often be understood mechanistically to the point where one can design a new catalytic molecule or material on the basis of established chemical principles. However, the activity and selectivity hinge on the details of complex kinetic phenomena, often at spectroscopically elusive active sites. There is consequently an element of empiricism in catalyst development. For this reason, catalysts are prime candidates for combinatorial chemistry. Following the early reports of combinatorial materials libraries by Schultz, Xiang, and co-workers,[3] the first reports of the development of combinatorial synthesis and screening methods for catalysts began to appear. The catalysts that have been studied combinatorially since then include transition metal complexes in which the ligands are systematically varied,[7] heterogeneous inorganic catalysts consisting of mixed metals,[8] supported metals,[9] and metal oxides,[10] and resin-bound organic catalysts, such as oligopeptides.[11]

This field is growing rapidly, and several comprehensive reviews devoted to combinatorial catalysis have recently appeared.[12] They underscore some of the challenges that

Handbook of Fuel Cells – Fundamentals, Technology and Applications, Edited by Wolf Vielstich, Hubert A. Gasteiger, Arnold Lamm. Volume 2: *Electrocatalysis*. © 2003 John Wiley & Sons, Ltd. ISBN: 0-471-49926-9.

exist in making and screening large libraries of catalysts. Parallel methods such as infrared (IR) thermography and colorimetric product detection allow for screening of very large libraries, but they give indirect information about the activity and selectivity of each catalyst. Other screening techniques, such as mass spectrometry and resonant multiphoton ionization (REMPI) give more direct information but in serial fashion. In all cases it is important to verify that the microscale fabrication and high throughput techniques used will give information that can be correlated with the performance of bulk catalysts under "real-world" conditions. With quantitative data from the screening of many large libraries, an unprecedented opportunity exists for discovering new correlations between catalyst composition, structure, and activity.[13] Towards this goal, the management and analysis of data has become an important issue. The methods for mapping and analyzing the results from large parameter spaces, which have become increasingly sophisticated, have been reviewed recently.[12c]

Electrocatalysts present a special opportunity and also a difficult problem for combinatorial research.[14] Electrocatalysts in combinatorial libraries are part of an electrochemical cell. This means that the powerful tools of electrochemical analysis (steady-state and dynamic voltammetry, chronoamperometry, scanning electrochemical microscopy, spectroelectrochemistry, complex impedance analysis) can be directly applied to the problem. This provides a new handle, both for screening and for subsequent kinetic/mechanistic studies, that is not available in nonelectrochemical catalyst research. The problem with electrocatalysis is that it occurs at an electrode/electrolyte interface. In the case of fuel cells, this is a three-phase interface between a liquid or gaseous fuel, a solid polymer electrolyte, and a nanophase metal catalyst. The metal catalyst must also be connected to the external circuit. Much of fuel cell electrocatalysis research is concerned not with improving the metallic catalyst per se, but with optimizing its interfacial contact and utilization in a complex material system (see Section 3.9). Combinatorial discovery methods must acknowledge this fact, and special care must be taken to compare the results of any screening process with the performance of bulk catalysts in real fuel cells.

1.3 Fuel cell anode and cathode reactions

Fuel cells operate by oxidizing a fuel (hydrogen, CO, ammonia, or organic molecules) at the anode and reducing oxygen at the cathode. Because combinatorial methods have so far been used to identify catalysts for polymer electrolyte membrane (PEM) fuel cells, we will focus here on reactions that occur in these cells.

The most common anode reaction for PEM fuel cells is the oxidation of hydrogen, equation (1), often accompanied by oxidation of CO, equation (2), if the hydrogen is produced by reforming an organic fuel:

$$H_2(g) \longrightarrow 2H^+(aq) + 2e^- \quad (1)$$

$$CO(g) + H_2O(l) \longrightarrow CO_2(g) + 2H^+(aq) + 2e^- \quad (2)$$

The hydrogen oxidation reaction is kinetically facile at Pt-catalyzed electrodes, but is inhibited by the adsorption of CO. A second anode reaction, which occurs in direct methanol fuel cells (DMFCs), is the oxidation of methanol:

$$CH_3OH(aq) + H_2O(l) \longrightarrow CO_2(g) + 6H^+(aq) + 6e^- \quad (3)$$

Because this is a six-electron reaction, it is mechanistically complex and kinetically slow. Substantial effort has been devoted to optimizing catalysts for this reaction.

The cathode reaction in PEM fuel cells is the reduction of oxygen to water:

$$O_2(g) + 4H^+(aq) + 4e^- \longrightarrow 2H_2O(l) \quad (4)$$

As it is a four-electron process, this reaction is also the source of significant polarization losses in PEM fuel cells. Consequently, a significant effort has also gone into researching and optimizing different classes of cathode catalysts.

1.4 Heuristic models for predicting catalyst compositions

Traditionally, the search for better heterogeneous catalysts proceeds from a model or an understanding of the mechanism of the reaction at the catalyst surface. This is obviously a sensible way to approach the problem if the preparation and testing of new catalyst compositions is time-consuming and expensive, because it focuses on the likely solutions to the problem and eliminates many possibilities that do not make sense chemically.

A good example of this approach is the development of platinum alloy catalysts for methanol oxidation, reaction (3). Pure Pt is a poor catalyst for the reaction, because it is rapidly poisoned by CO, a surface-bound intermediate in methanol oxidation. Adatoms and alloying elements such as Ru and Sn cause Pt to oxidize methanol at much lower overpotentials,[15–21] and several models have been proposed to explain this effect. One of these – the bifunctional mechanism – proposes that water (which is needed in reaction (2)) can be bound more efficiently by oxophilic metals that alloy with or physically contact

nanoscale grains of Pt.[22–24] A second model involves a "ligand effect", in which the d-band occupancy of Pt is changed by alloying elements, lowering the activation barrier for CO oxidation.[25–28] A third model, more recently proposed, claims that elements such as Ru and Os do not alloy with Pt, but provide a mixed-conductor hydrous oxide phase that improves contact between the Pt surface and the polymer electrolyte.[29]

Although none of these models is predictive in a quantitative way, each carries an implicit prescription of where to look for better catalysts. For example, the bifunctional model suggests that oxophilic elements such as Ru, Os, Sn, W, and Mo will accelerate reaction (2).[30] Ley *et al.*, tested this idea by examining ternary Pt-Ru-Os compositions that lay within the face-centered cubic single phase region of the ternary alloy phase diagram.[31] They were able to correlate the effectiveness of alloying elements with metal–oxygen bond strengths, to rationalize why Ru is a more effective alloying element than Os, and to show that ternary combinations give higher activities than simple binaries. Similar reasoning led to the search for better anode catalysts for reformate-air fuel cells among binary and ternary combinations of Pt, Ru, Mo, and W.[32, 33]

This kind of chemical intuition is also important for combinatorial catalyst discovery because the universe of possible combinations is so vast that it cannot be covered in a reasonable amount of time, even with very high throughput synthesis and screening methods. At present, one can make arrays of tens or hundreds of different catalysts, which are typically tested over a period of several days. It is informative to consider how this number compares with the number of possibilities if the search is not constrained by heuristic models. For an $n-1$-dimensional simplex-type combinatorial map of n different components,[34] the number of combinations N is given by the equation

$$N(n,m) = \frac{(n+m-2)!}{(n-1)!(m-1)!} \qquad (5)$$

in which m is the number of compositions along a given binary edge in the map. Figure 1 illustrates this mapping strategy with a three-dimensional, $n = 4$ map, and shows how it can be "unfolded" into a two-dimensional array. The map in Figure 1 has 10 different compositions along any binary line ($m = 10$) and four components ($n = 4$), so $N = 12!/(3!9!) = 220$. An array of this size can be easily synthesized and screened, as described in Sections 2.1 and 2.2. However, if one wishes to use 16 components at the same resolution, then $N = 1\,307\,504$, and for 30 components (the number of transition elements in the periodic table) there are over 10^8 possibilities. This number can be reduced substantially if the search is narrowed to eliminate

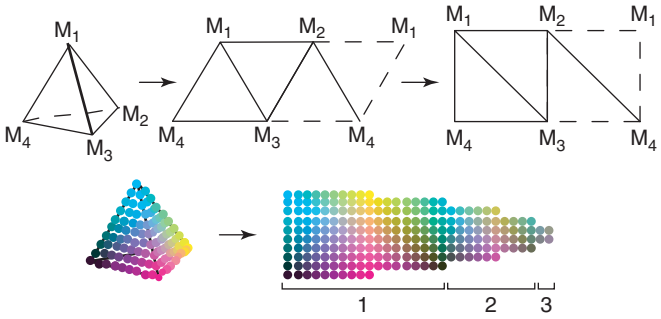

Figure 1. Unfolding of a three-dimensional, 220-member compositional map into two dimensions. The four elements are represented as cyan, magenta, yellow, and black dots, and mixtures as mixtures of these colors. Dashed lines represent redundant binaries that are eliminated in the map, and the three concentric shells are indicated by numbered brackets. Shell 1 consists of elements, binaries, and ternaries. Shells 2 and 3 contain quaternary combinations. (Reprinted from Reddington *et al.* (1998)[40] with permission from the American Association for the Advancement of Science.)

combinations of more than 3–4 elements in a given catalyst. For example, for $n = 30$ and $m = 5$, there are about 40 000 possibilities, which represent combinations of one, two, three, and four elements at a resolution of five compositions (100/0, 75/25, 50/50, 25/75, 0/100) along each of the binary lines in the 29-dimensional composition space. At such low resolution, however, the search could miss many active phases, even if it were possible to make and screen such a large number of catalysts within a reasonable period of time. A compromise position is to cover the most likely combinations suggested by heuristic models, while allowing enough variability to make discoveries "out of the box" as well.

1.5 Comparison of combinatorial and serial methods for catalyst discovery

The traditional method for optimizing fuel cell catalysts is to formulate them individually, make individual membrane electrode assemblies, and test them one at a time, usually by acquiring steady-state current–voltage data in a dedicated test stand. These measurements are often coupled to detailed characterization of the individual catalysts by methods that include electron microscopy, X-ray powder diffraction (XRD), X-ray photoelectron spectroscopy (XPS), and gas physisorption/chemisorption measurements. This approach allows one to correlate the dispersion of the catalyst, the oxidation states of elements on its surface, and the crystalline phases present with catalyst activity. A meaningful comparison of the activity of different porous catalysts cannot be made without surface normalization (see

Normalization of porous active surfaces, Volume 2 and **Rotating thin-film method for supported catalysts**, Volume 2). In situ spectroscopic techniques such as infrared spectroscopy and X-ray absorption spectroscopy (XAS) can also provide useful information about the nature of adsorbed molecules such as CO and changes in the oxidation states of metals that occur in the fuel cell.

While serial testing and characterization are slow – often requiring weeks or months for detailed study of a single catalyst – it offers the advantage of being a "real-world" test under true operating conditions. Catalyst performance is notoriously sensitive to the details of membrane electrode assembly (MEA) preparation and testing, and these problems are not considered in most combinatorial studies. Serial testing in MEAs also allows one to prepare high surface area catalysts by ex situ methods that are not easily adapted to a high throughput format. For example, in the Adams method,[35] catalyst precursors are synthesized as fine oxide particles in a nitrate flux; the active, metallic form of the catalyst is actually generated in situ in the MEA during conditioning. Some solution-phase preparative methods[36–38] require large reaction volumes or heating/stirring/filtration steps that cannot easily be performed in the micro-well or planar array format of the typical combinatorial experiment.

The advantage offered by combinatorial testing is speed, and this allows one to look systematically at a broad spectrum of catalysts. In general, the composition is varied across an array of catalysts. Alternatively, other parameters (such as synthetic conditions) can be treated as combinatorial variables.

2 COMBINATORIAL METHODS FOR ELECTROCATALYSIS

2.1 Optical screening of electrocatalysts

Indirect optical detection of electrochemical half-cell reactions was the first high throughput screening method applied to fuel cell catalysts. This method was originally developed to search for improved DMFC anode catalysts.[39] Since then it has been applied to problems involving PEM fuel cell anodes[40] and cathodes,[41] electrolyzers,[42] amperometric sensors,[43] and photoredox reactions.[44]

2.1.1 Fluorescence techniques

The optical screening method is based on the idea that all electrochemical half-cell reactions generate or consume ions in order to maintain charge neutrality. Anode reactions such as (1)–(3) generate protons, and cathode reactions such as (4) consume protons. Other reactions, such as oxidation of metals or halide ions, generate or consume other anions and cations. If a chemosensor[45] – an indicator molecule for the particular ion of interest – is present, then its change in absorbance or emission pinpoints the location – usually a set of individual spots in a catalyst array – where the half-reaction is occurring. Typically, fluorescence is preferred over absorbance as a detection method because of its greater sensitivity. The advantages of this screening method are its simplicity, since it requires only aqueous indicator solutions and a hand-held ultraviolet (UV) lamp, and the fact that it is an intrinsically parallel technique. One drawback is that the method is indirect. It does not allow one to measure current directly; however, fluorescence images can be taken at a number of potentials to give a qualitative $I-V$ characteristic for the spots in a catalyst array.

Figure 2 illustrates the optical screening method with a small ternary array of Pt/Rh/Os DMFC anode catalysts supported on a Toray carbon electrode. In this case quinine ($pK_a = 5.5$), an acid-sensitive fluorescent indicator, provides a pH map of the array. At low overpotential (center frame), one spot shows the brightest fluorescence, and is ringed around by six less active spots. This region contains the best methanol oxidation catalysts in the array. The image at the right illustrates the fact that at sufficiently high overpotentials all the catalyst spots in the array are active.

Because PEM fuel cells operate under very acidic conditions, fluorescent indicators that turn on at low pH values are most useful. The Ni^{2+} complex of PTP **(1)**, which is acid-fluorescent with a pK_a of 1.5, has been used as an indicator for anode reactions (1)–(3)[40, 41] and for water oxidation by electrolyzer anode catalysts.[42] Phloxine B **(2)**, which is fluorescent in its basic form and has a pK_a of 2.7,

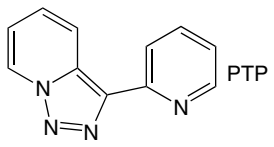

(1)

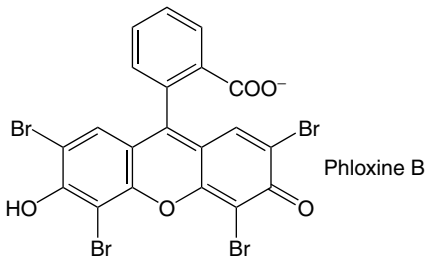

(2)

Figure 2. An array of 28 Pt/Rh/Os catalyst spots in 6 M aqueous methanol, pH 6, quinine indicator. (a) image in white light; (b) fluorescence image at low overpotential; (c) fluorescence image at high overpotential, where methanol oxidation occurs at every spot in the array. (Reprinted from Reddington *et al.* (1998)[40] with permission from the American Association for the Advancement of Science.)

has been used as an indicator for cathode reaction (4).[40, 42] Other indicators should be used when the intended use of the catalyst is at more basic pH. For example, quinine has been used as an indicator for glucose oxidation,[43] because glucose sensors and bio-fuel cells utilizing glucose operate near physiological pH.

2.1.2 *Array synthesis and characterization*

The optical method can be effective with very large arrays, because individual addressing is not required and because fluorescence is easily resolved from small spots. The size and quality of the catalyst array are limited by the preparation method. Initially, these arrays were fabricated by hand-pipetting[39] or by ink-jet printing[40] metal salts in the appropriate ratios on to Toray carbon, a porous matte of carbon fibers that is used as a backing layer for MEAs in PEM fuel cells. The metal salts are reduced to their active forms by using aqueous sodium borohydride[46] or hydrogen gas. More recent experiments have employed 715-member arrays that contain combinations of five elements. These arrays are made by using a commercially available robotic plotter (Figure 3) to deposit metal salt solutions. The plotter can be used to generate arrays of unsupported or supported catalysts at loadings comparable to those used in PEM fuel cells. The spot diameter in these arrays is typically 2–4 mm.

Data are acquired from these arrays in the form of fluorescent maps as a function of applied potential for the reaction of interest. The planar activity map can be "re-folded" into a multidimensional diagram, allowing zones of activity to be imaged. Figure 4 shows an example of such a map for a quaternary array of water oxidation catalysts. It is apparent in the map that there are two major zones of activity centered on the Pt/Ir/Os and Pt/Ir/Ru ternary faces.

An important component of all combinatorial experiments of this type is to characterize representative catalyst spots on the array and then compare them with bulk quantities of catalysts made by the same or other methods. A first step in this process is to verify the presence of the intended elements in the catalyst spots and to determine that a single composition gives a uniform response across the entire array. Beyond this, it is important to recall that the performance of a catalyst synthesized by microscale methods may be irrelevant to that of catalysts of the same nominal composition in an MEA. This is because catalyst utilization is sensitive to the way the catalyst is synthesized and to the way the MEA is fabricated. Our experience is that this is particularly true for supported catalysts. For example, the hydrophobicity of carbon-supported anode and cathode catalysts for reformate-air fuel cells must be carefully controlled, because flooding by water blocks access to the catalyst surface. If the screening of an array of

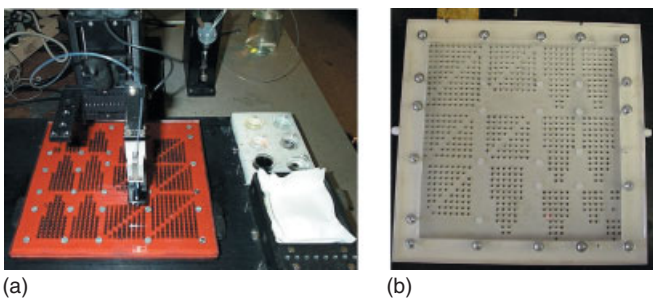

Figure 3. (a) robotic delivery of metal salt solutions to a 715-well pentanary array. A Toray carbon sheet is sandwiched between flexible gaskets (red) which define the wells. (b) top view of a screening cell for 715-member electrode arrays.

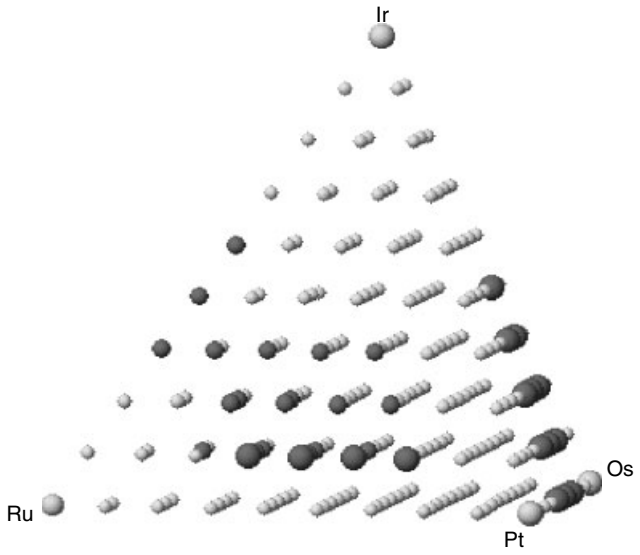

Figure 4. Re-folded activity map for oxygen evolution from a quaternary array of Pt/Ru/Os/Ir catalysts on Toray carbon paper. Large and small gray spheres indicate the onset of Ni-PTP fluorescence at +1350 and +1400 mV vs the normal hydrogen electrode (NHE), respectively.

these catalysts is carried out in a liquid indicator solution, however, more hydrophilic supported catalysts appear to have higher activity[47]. The bottom line is that claims of catalyst "discoveries" must be verified by fuel cell testing in order to eliminate false positives and negatives.

2.2 Electrochemical screening of electrocatalysts

The fluorescent screening method has some limitations that can be overcome by making direct electrochemical measurements on an array of catalysts. Fluorescent detection generally requires a liquid electrolyte, an unbuffered solution, and a temperature that is compatible with the operation of the fluorescent dye. In contrast, a PEM fuel cell contains a polymer electrolyte and is often run at 60–90 °C. Also, the fluorescent response, which is semi-quantitative, has lower information content than methods that give a full $I-V$ characteristic for each catalyst. Several such methods, based on array electrochemical cells and scanning electrochemical probes, have now been reported.

2.2.1 Array electrochemical systems

Electrochemical array cells for screening electrocatalysts were developed independently by Ward and co-workers[48] and by Warren *et al.*[49] The two systems were quite similar, with square grids of 64 individually addressable microelectrodes fabricated on silicon wafers by lithographic methods. Address lines contacting the individual working electrodes were insulated by dielectric layers, leaving only the Au or Pt working electrodes exposed to the electrolyte solution. Figure 5 shows an example of such a working electrode array.

Ward *et al.* examined the electrochemical response of Au electrodes modified by alkanethiol self-assembled monolayers using cyclic voltammetry. They were able to show a good correlation between the rate of electron transfer to solution-phase redox couples (by cyclic voltammetry of the working electrode array) and the optical fluorescent response using fluorescein as an indicator. Warren *et al.* electrodeposited Pt/Ru films on to an array of Pt electrodes and were able to confirm by potential step chronoamperometry that the most active composition for methanol oxidation (in 0.5 M H_2SO_4 solution) contained approximately 50 mol% Pt. Similar results had been obtained earlier by Chu and Gilman in a study of Pt/Ru catalysts of different compositions.[50]

A problem shared by both the optical and direct electrochemical screening methods described above is that the screening conditions are quite far from those used in the actual fuel cell. The catalyst contacts a liquid electrolyte, rather than a polymer electrolyte, and is often made by techniques (e.g., electrochemical deposition or reduction in microwells) that are not used in fuel cell MEAs. Additionally, fuel cell catalysts require conditioning, in which the MEA is run from hours to days after assembly of the fuel cell. In response to this problem, Liu *et al.* developed a parallel testing device (Figure 6) that contains 25 individually controllable microelectrodes.[51] The advantage of this array

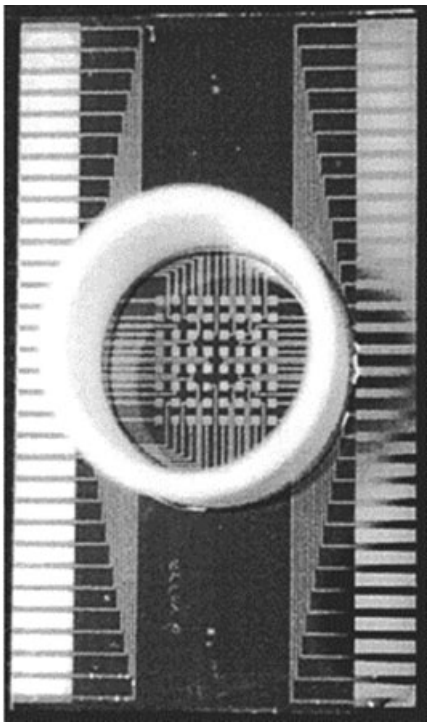

Figure 5. 64-working electrode array, with a 3 cm diameter Delrin cylinder forming the electrolyte compartment. (Reprinted with permission from Sullivan *et al.* (1999)[48] © American Chemical Society.)

Figure 6. 25-electrode cell for testing anode and cathode electrocatalysts. (a) shows an individual sensor electrode, which integrates into the flow field block shown on (b). 25 supported or unsupported catalysts are pressed into a single membrane electrode assembly and run against a common large area counterelectrode under desired conditions of temperature, fuel/oxidant flow rate, and stoichiometry.

cell is that each electrode is essentially a miniaturized fuel cell: gaseous fuel (or air) is introduced through realistic flow fields, and the catalyst/MEA layer is fabricated in exactly the same manner as in the actual cell.

This cell has been tested with a Nafion electrolyte membrane using several catalysts for methanol oxidation. The individual catalysts were prepared as inks and applied to ELAT carbon, which was cut into disks and hot-pressed into the Nafion membrane. Hydrogen was run at the common cathode in order to provide a large area, non-polarizable reference/counter electrode. Figure 7 shows the result of this study. At potentials negative of 0.4 V, there is a close coincidence of all the curves. However, at more positive potentials, the curves are increasingly affected by mass transfer and become almost entirely mass-transfer limited at approximately 0.8 V. The raw data may be mass-transfer corrected according to the equation[52]

$$\frac{1}{i} = \frac{1}{i_{\text{kinetic}}} + \frac{1}{i_{\text{limiting}}} \tag{6}$$

When this is done, there is excellent reproducibility for the same catalyst measured simultaneously at 25 individual working electrodes. An array containing four different catalysts also correctly reproduces the performance rankings obtained individually in large area PEM fuel cells. Again, while a ranking of intrinsic catalyst reactivities would require surface area normalization (see Section 3.8), the mass-normalized ranking shown in Figure 7 gives practical guidance about the performance of each of these catalysts in a working DMFC.

2.2.2 *Scanning probe methods*

Hillier and co-workers have recently introduced an interesting electrocatalyst screening method based on scanning electrochemical probes.[53] The method uses a scanning electrochemical microscope(SECM)[54] as a means of both imaging the electrode surface and probing its electrocatalytic activity. In related experiments, Kucernak and co-workers used SECM to obtain images of the local concentration of hydrogen above Pt catalyst particles dispersed on graphite[55].

When a conductive ultramicroelectrode tip is brought into close proximity with a macroscopic electrode surface, an electrochemical feedback loop is set up between the two conductive surfaces. If the feedback loop is established by using a fast, outer-sphere redox couple such as $Ru(NH_3)_6^{3+/2+}$, the image generated by rastering the probe tip does not distinguish between catalytic and non-catalytic parts of the surface. However, if the tip performs an inner-sphere reaction such as reduction of H^+ ions, then catalytically active regions of the surface (which generate H^+ through reactions (1) or (3), for example) show higher feedback current. To date the technique has been used to map the catalytic activity of a Pt coverage gradient on a conductive indium tin oxide (ITO) substrate, to image Pt electrode arrays, and to study the potential dependence and dynamics of Pt catalyst poisoning by CO. Because of its high spatial resolution, and because it is not necessary to fabricate individual address lines to each spot on the electrode array, this method is potentially useful for screening large arrays of electrocatalysts.

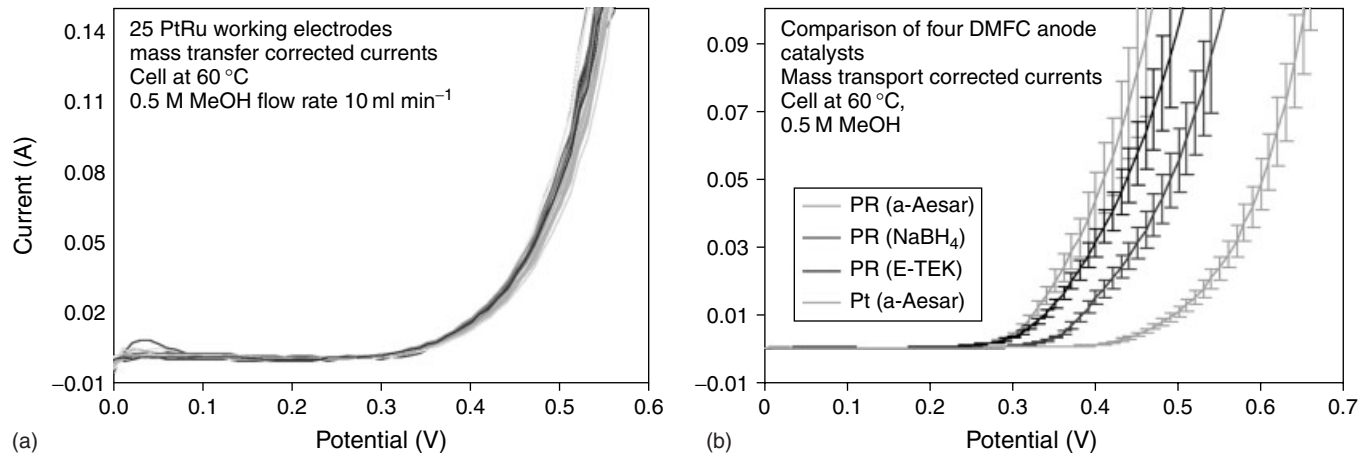

Figure 7. (a) mass transfer corrected anode $I-V$ curves for 25 electrodes using an unsupported Johnson-Matthey Alfa-Aesar Pt/Ru (50 : 50) catalyst. (b) activity comparison for four DMFC anode catalysts. The average mass transfer corrected current of six spots is shown for each of the four catalysts. The area of each circular catalyst spot was 0.71 cm^2, and the metal loadings were 3.97, 4.24, 4.15, and 4.97 mg cm^{-2} for Johnson-Matthey Alfa Aesar Pt/Ru (50 : 50), $NaBH_4$-prepared Pt/Ru (50 : 50), E-TEK Pt/Ru (50 : 50), and Johnson-Matthey Alfa Aesar Pt, respectively.

3 COMBINATORIAL DISCOVERY OF ELECTROCATALYSTS

3.1 Platinum alloy catalysts for direct methanol fuel cell anodes

The optimization of electrocatalysts for methanol oxidation has been intensively studied for nearly 40 years.[15–33, 50, 56, 57] DMFCs offer the attractive advantage of utilizing a liquid, high energy density fuel, but they suffer from severe polarization losses, particularly at the anode. MEAs for DMFCs are usually prepared with unsupported Pt/Ru anode catalysts because the reaction rate is so slow that it is advantageous to maximize the amount of catalyst in contact with the polymer electrolyte. The discovery of anode catalysts that could operate at lower loading of precious metals and at higher current density would greatly enhance the viability of DMFCs for a variety of applications.

Reddington *et al*.,[40] building on an earlier report that added Os enhances the activity of Pt/Ru catalysts,[31] examined combinations of Pt, Ru, Os, Ir, and Rh in quaternary arrays by the fluorescent screening method.[40] The choice of Ru and Os as alloying elements was suggested by the bifunctional model. Ir and Rh, which are not oxophilic elements, were not expected to be particularly good additives. Interestingly, the most active compositions in the screening experiments all contained small amounts of Ir or Rh, although the Rh-containing catalysts tended to be unstable. Follow up studies showed that the optimum concentration of Ir in bulk catalysts prepared by borohydride reduction was 4–6 mol%.[58] This corresponds approximately to the solubility limit of Ir in the face-centered cubic (fcc) Pt alloy phase. Although the most active catalysts found had relatively low Pt content (37–50 mol%), XRD analysis suggested that the fcc phase was enriched in Pt. This is consistent with studies of arc-melted Pt/Ru alloys that show an optimum Pt content of about 70 mol%.[59]

Gorer and co-workers at Symyx, Inc., studied Pt/Ru/Pd ternaries as methanol oxidation catalysts in multielectrode arrays.[60] The arrays were prepared by electrodeposition from sulfuric acid solutions of H_2PtCl_6, $RuCl_3$, and $PdCl_2$, and the composition of representative alloys was determined by X-ray fluorescence. Chronoamperometric experiments in 1 M methanol/0.5 M H_2SO_4 solutions showed enhanced current with added Pd, relative to Pt/Ru binary compositions, with the optimum composition containing about 30 mol% Pd. Although these preliminary results are interesting, they have not yet been followed up with detailed characterization of the catalyst structure, and the catalysts have not been tested against commercial Pt/Ru catalysts in actual fuel cells.

3.2 Cathode catalysts for polymer electrolyte membrane fuel cells

Cathode catalysis is another important problem for PEM fuel cells. The cathode represents the largest source of polarization loss in hydrogen–air fuel cells and also adds substantially to losses in reformate-air fuel cells and DMFCs. In addition, in DMFCs the crossover of fuel from the anode side, through the semi-permeable polymer electrolyte membrane, creates a mixed potential at the cathode which further degrades cell performance.[61–63]

Pt is the most widely used cathode catalyst in PEM fuel cells, and some efforts to improve it have focused on alloys that prevent an insulating anodic film, probably consisting of adsorbed OH, from inhibiting oxygen reduction. Alloys with 3d elements have been studied, with Fe, Co, and Cr showing the greatest tendency to inhibit OH adsorption.[64–67] Other work has concentrated on finding substitutes for Pt that are "methanol tolerant," meaning that they are less susceptible to the deleterious effects of fuel crossover.[68–72]

Strasser and co-workers used the array electrode method to study the effects of alloying 3d elements with Pt.[73] Thin-film electrode libraries were made by sputter deposition of the elements. They found active Pt/Fe binary and Pt/Co/Cr ternary compositions, as anticipated from earlier work on high surface area catalysts.[64–67] Other active catalysts with apparent activities higher than that of Pt/Co/Cr were also found in the screening experiments, but their compositions have not yet been disclosed. A representative ternary composition (Pt : Co : Cr atomic ratio 50 : 25 : 25) was synthesized in scaled-up form as a carbon-supported catalyst and was tested by rotating disk voltammetry. Potential step chronoamperometry showed higher cathodic current for this composition, relative to Pt/C. A Tafel analysis of these electrodes was quite informative. Pure Pt/C gave a reduced Tafel slope at high potentials, whereas the carbon-supported alloy maintains a slope of 120 mV per decade. The reduced Tafel slope has previously been identified with the formation of an anode film on Pt.[64, 74]

3.3 Ruthenium alloy methanol-tolerant cathode catalysts

Methanol-tolerant, non-noble metal catalysts were first discovered about 15 years ago by Alonso-Vante, Tributsch, and co-workers.[68–70, 72] The most active of these materials

contain ruthenium and selenium doped with molybdenum and other elements. These ruthenium-rich compositions were originally formulated as Chevrel (M_6X_8) phases or M_2X (M=Ru or Mo) compounds, and later as $Ru/Ru_xSe_yC_vO_w$, in which the active $Ru_xSe_yC_vO_w$ phase is supported on nanocrystalline Ru.[71] Because substantial uncertainty exists about the structure and composition of the active catalysts, this class of materials represents and interesting case for combinatorial optimization.

These materials were examined by the fluorescent screening method, using Phloxine B as the indicator.[41, 75] Ru/W/Sn/Se/Mo combinations were printed on to Toray carbon paper using aqueous glycerol inks (solutions of $RuCl_3 \cdot xH_2O$, SeO_2, Na_2WO_4, $SnCl_4$, and Na_2MoO_4) and then reduced with hydrogen gas at 250 °C. Active compositions in 645-member arrays were found in the Ru-rich regions of the Ru/Sn/Se ternary and Ru/Mo/Sn/Se quaternary regions. Physical characterization of the most active composition, $Ru_{7.0}Sn_{1.0}Se_{1.0}$, by powder X-ray diffraction, gas adsorption, and X-ray photoelectron spectroscopy, revealed that the predominant crystalline phase was hexagonal close-packed (hcp) ruthenium, and showed a surface mostly covered with oxide, consistent with recent studies by Tributsch *et al*.[72]

Preliminary MEA testing of carbon-supported catalysts prepared by the same method showed that they are poor catalysts, relative to Pt metal, but that they have the expected methanol tolerance. It should be noted that the synthetic method used to prepare these catalysts was chosen for convenience to be compatible with ink-jet printing techniques. More sophisticated routes to metal chalcogenide catalysts, based on organometallic precursors, have been developed.[72] A logical extension of this preliminary work would be to adapt these preparative methods to combinatorial screening.

3.4 Dual use catalysts for regenerative fuel cells

Regenerative PEM fuel cells that can perform both as a fuel cell and an electrolyzer promise to be very efficient energy conversion and storage devices for both space and terrestrial applications. These systems usually have one electrode for oxygen evolution and reduction, and another electrode for the corresponding hydrogen reactions. With favorable kinetics at the hydrogen electrode, the key issue in these systems is the development of more active and stable bifunctional catalysts for the oxygen electrode.

The optimization of catalysts for two different reactions (oxygen reduction and water oxidation) presents a problem that is not easily addressed by serial methods. With combinatorial screening, one can obtain a full activity map for each reaction, and then combine them to produce a consensus map. Chen *et al*. used this approach to find optimized unsupported and supported catalysts from combinations of Pt, Ru, Ir, Os, and Rh.[42] Figure 8 shows quaternary activity maps for catalysts supported on Ebonex, a conductive titanium oxide containing Ti_4O_7 and other phases. The consensus map shows a relatively narrow region of high activity on the Pt/Ru/Ir ternary face, near the Pt/Ru binary edge.

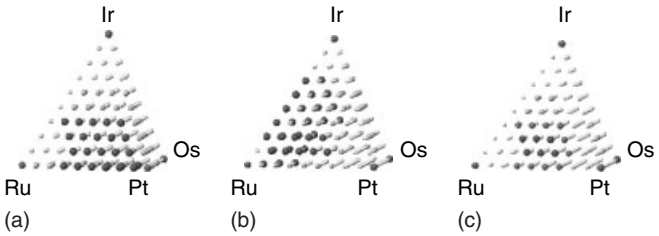

Figure 8. Activity maps for oxygen reduction (a), water oxidation (b), and a consensus map (c) for both reactions for Ebonex-supported Pt/Ru/Ir/Os.

Interestingly, the addition of small amounts of Ir stabilizes Pt/Ru against anodic corrosion, and the ternary has significantly higher catalytic activity than the stable Pt/Ir binary. A detailed kinetic comparison of anodically stable catalysts $Pt_{4.5}Ru_4Ir_{0.5}$ and Pt_1Ir_1 showed that the addition of the oxophilic element Ru increases the reaction rate by stabilizing S–O bonds (S ≡ surface atom) and accelerating the oxidative deprotonation of S–OH groups.

3.5 Electrocatalysts for amperometric glucose sensors

Amperometric sensors are widely used to detect glucose levels in blood. Most glucose sensors are based on glucose oxidase, which catalyzes the oxidation of glucose in the presence of oxygen. While these enzyme electrodes have excellent specificity, they require frequent calibration because of the poor durability of the enzyme. The electro-oxidation of glucose on noble metal surfaces has been studied in the hope that an effective enzyme-free sensor could be made.[76, 77] Pt and Au electrodes are readily poisoned by chemisorbed intermediates in the oxidation reaction. However, adatoms of Bi, Tl, and Pb enhance the electroactivity of Pt in glucose solutions.[78, 79]

This problem was studied in combinatorial electrocatalyst arrays by Sun *et al*.[43] They screened 715-member arrays containing combinations of Pt, Pb, Au, Pd, and Rh, by the fluorescence method and found a number of active

unsupported alloys containing both Pt and Pb. In tests of bulk carbon-supported catalysts, Pt_2Pb/C and related alloys catalyzed glucose oxidation at substantially more negative potentials than Pt/C. These catalysts were also insensitive to potential interferents (ascorbic and uric acids and 4-acetamidophenol), which are oxidized at slightly more positive potentials, but were sensitive to chloride poisoning. Rotating disk electrode experiments showed that the improvement in catalytic performance could be attributed to inhibition of the adsorption of glucose oxidation products.

4 CLOSING THE LOOP ON DISCOVERY — FOCUS TESTING AND CHARACTERIZATION

Apart from the obvious practical application of finding improved catalysts, the combinatorial method has the potential to provide systematic information on reactivity as a function of composition and other parameters. When coupled with structural phase mapping of the parameter space and detailed kinetic studies, the data can be used to augment or refine the heuristic models that were used to design the search. This creates a feedback loop for gaining new mechanistic insight into catalytic reactions and then using it to decide where to look next for improved catalysts.

4.1 Phase identification and structural characterization

Fuel cell catalysts are typically carbon supported for reformate fuel cells and unsupported in the case of liquid feed fuel cells such as DMFCs. Although carbon-supported catalysts have been observed to have higher specific activities ($mA\,mg^{-1}$) than unsupported catalysts in DMFCs, mass transport effects limit use of unsupported catalysts in liquid feed fuel cells with sluggish kinetics.[80] The requirement for very high metal dispersion and the volatility of oxides of key alloying candidates such as Ru, Os and Mo restricts the synthesis of mixed metal catalysts to low-temperature preparative methods. Thus fuel cell catalysts, as prepared, are often phase-segregated materials consisting of Pt-rich alloy phase(s) in combination with other metallic or oxide phases.[58, 81]

Pt/Ru anode catalysts provide a good example of the complexity of phase behavior found with fuel cell catalysts. Gurau *et al*. reported that the lattice parameters (fcc) of high surface area mixed metal catalysts containing Ru were larger than those observed with arc-melted alloys of the same composition.[58] They explained these results as phasing out of some of the smaller Ru atoms from the alloy phase leaving a Pt-rich alloy with a correspondingly larger lattice parameter. Dinh *et al*., conducting in situ CO stripping experiments with Pt/Ru DMFC anode catalysts, concluded that the most active catalysts contained metallic Pt/Ru alloy particles.[82] In contrast, Rolison and co-workers proposed that in DMFCs, the active electrocatalyst for methanol oxidation is not a bimetallic alloy but a mixed phase containing Pt metal and hydrous ruthenium oxides (RuO_xH_y).[29] O'Grady *et al*.[83] studied the structure of Pt/Ru catalysts using X-ray absorption and concluded that in the potential window where methanol oxidation occurs, the metal oxides were reduced to their metallic form. Similarly, in a series of recent papers using in situ extended X-ray absorption fine structure spectroscopy (EXAFS), Russell and co-workers concluded that for a well-mixed Pt/Ru/C electrocatalyst the Pt and Ru are both metallic in nature, and exist as bimetallic alloys.[84, 85]

In situ X-ray absorption near edge structure (XANES) experiments were performed on a working reformate-air fuel cell to study the structure of carbon supported Pt/Ru anode electrocatalyst. The fuel cell was operated in a normal mode without the use of supplemental electrolytes. The in situ Pt L_{III}-edge and Ru K-edge XANES of the fuel cell MEAs showed metallic characteristics under all operating conditions. These results demonstrate that under the reducing conditions of normal fuel cell operation, the Pt/Ru catalyst exists as (a) metallic phase(s).[86] It is not unexpected that reformate catalysts are metallic since the higher temperature operation requires less polarization of the anode catalysts.

The important lesson for combinatorial analysis in this case is that phase identification is not a trivial issue, since the best catalysts may consist of several phases (in addition to the support). Which phases are present depends on the method of preparation, as well as on the electrochemical history of the catalyst. There clearly exists a need for high throughput structural characterization techniques that could complement the fast synthesis/screening methods that have been reported to date for electrochemical arrays. Ideally, one could obtain phase maps and correlate them with activity maps as a function of composition and preparative conditions.

4.2 Reaction kinetics and mechanisms

The typical model for combinatorial discovery is to use rapid synthesis/screening methods to identify leads (the "discovery" phase of the problem) and then to use slower but more reliable methods for full testing and characterization. Once the search has been narrowed to a small number

of interesting compositions, it is instructive to ask what, if anything, has changed with the new catalyst in the mechanism of the reaction.

This approach has been applied to DMFC anode catalysts by Gurau *et al*.[57] Combinatorial screening identified quaternary Pt/Ru/Os/Ir catalysts that had significantly higher activity than Pt/Ru or Pt/Ru/Os prepared by the same method. The "oxophilicity" hypothesis (implicit in the bifunctional mechanism) failed to explain the improved performance obtained by adding Ir, because the Ir–O single bond is weak ($410 \pm 40\,\mathrm{kJ\,mol^{-1}}$) compared with Ru–O and Os–O bonds (530 ± 40 and $600 \pm 80\,\mathrm{kJ\,mol^{-1}}$, respectively).[87] From reaction order plots, Gurau *et al*. postulated that the rate-determining step with the improved catalysts was not water activation, but activation of the methanol C–H bonds. Subsequent spectroscopic and theoretical work has supported this hypothesis. A potential-dependent XPS study of arc-melted alloy electrodes showed that at potentials relevant to fuel cell operation, surface Os atoms are less oxidized than Ru atoms in Pt/Ru/Os.[88] Density functional theory calculations suggest that Os may also serve as a C–H activator.[89] These studies support the idea that the role of Os and Ir is to accelerate C–H bond breaking.

Recently, concentration-dependent current–voltage curves together with CD_3OH and CH_3OD kinetic isotope data have shown unambiguously that C–H bond activation becomes a kinetically comparable effect within the fuel cell relevant potential regime for two high-performance mixed metal catalysts (PtRu and PtRuOsIr).[90] At potentials above 0.4 V, C–H activation becomes the dominant barrier to methanol oxidation. This result could be of practical importance because anode potentials between 0.4 and 0.5 V versus a dynamic hydrogen electrode (DHE) will be well within the DMFC operating potential window when low crossover membranes are developed. The inclusion of C–H bond activation as a possible rate-determining step also has implications for future catalyst discovery, since it suggests an expansion of the composition space to include C–H activator elements.

4.3 Optimizing the synthesis

One of the most significant problems with combinatorial catalyst discovery is the interplay between synthetic variables and composition. Two effects are of importance here: the ubiquitous presence of nonequilibrium phases and the problem of adapting the best synthetic techniques to high-throughput formats.

Because catalyst preparations are intended to give high surface area materials, the product is invariably a nonequilibrium phase or mixture of phases. For example, it has been established that for methanol oxidation, the optimum concentration of Ru in arc-melted Pt/Ru alloys is about 30 atom%.[59] However, for high surface area catalysts, which are not true alloys, the best concentration is approximately 50%. The phases obtained depend on the method used to prepare the catalyst. Consequently, different synthetic methods will identify different "optimum" compositions and false negatives are possible in combinatorial screening experiments.

Some of the best synthetic methods are specific to certain compositions, or to a rather narrow range of compositions. For example, the Watanabe method involves the oxidation of a platinum sulfite complex to colloidal PtO_2, mixing with $RuCl_3$ and base to form a mixed Pt/Ru oxide colloid, and reduction with hydrogen to give very active, high surface area Pt/Ru.[38] Because the colloid chemistry is specific to Pt and Ru, this method is not easily adapted to use with mixtures of other elements. Also, because this and other optimized synthetic methods involve large volumes of solutions, lengthy heating and stirring cycles, and filtration, they are not easily adapted to the preparation of large libraries of compositionally varied catalysts. Although in principle synthetic conditions can be considered one of the variables in a combinatorial screening experiment, in practice very little has been done to address the poor connection between the methods used to prepare catalyst libraries and those used to make good catalysts in bulk form.

5 CONCLUSIONS AND OUTLOOK

It is evident from the preceding sections that while combinatorial methods have now been applied to a range of problems in electrocatalysis, they have yet to produce revolutionary advances. In many cases the improvements claimed are difficult to assess precisely, because screening experiments have not been followed up with detailed testing of catalysts under "real-world" conditions. One of the difficulties with research on PEM fuel cells, which has yet to be addressed in high-throughput synthesis/screening experiments, is the strong interdependence of catalyst and MEA preparation techniques and catalyst composition and performance. To date most combinatorial arrays of catalysts have been made by convenient plotter, electrochemical, or vacuum deposition techniques. The synthesis has been applied to a broad range of compositions indiscriminately, even though it may be inappropriate for large ranges of composition space. This implies that many of these experiments will be dominated by false negatives. Likewise, the screening has been done in liquid electrolytes, often at ambient temperature even though the catalyst is intended to be used under quite different conditions.

There now exists a challenge and a good opportunity for this field to become more sophisticated by combining state-of-the-art synthetic methods with high-throughput testing under more realistic conditions. Both the fluorescence and array electrochemical methods give reasonably high throughput for catalyst testing, and the rate-determining step (with better preparative methods) will likely become the synthesis and analysis of catalysts. In this case, array methods can still be used to significant advantage to obtain parallel data sets for the same catalyst or for a smaller number of catalysts simultaneously.

Another important opportunity that exists in the field is to use high throughput electrochemical methods as a way of testing or refining models of catalytic reactivity. By comparing activity maps with compositional phase diagrams, we acquire another tool to understand which phase or phases are involved in the reaction. Unexpected discoveries (e.g., the enhancement of Pt/Ru/Os DMFC anode catalysts by small amounts of Ir, or the improvement of glucose oxidation catalysts by alloying Pt with Pb) force one to re-examine models for the catalytic reaction. When combined with detailed kinetic and structural studies, these discoveries can often lead to new insight into the mechanism of the electrode reaction. In this regard, there exists a need to adapt analytical techniques that are used to characterize individual electrocatalysts (such as X-ray diffraction and spectroelectrochemistry) to large arrays.

Finally, it is important to note that combinatorial methods have been applied to electrochemical problems for only a short period of time and several important classes of reactions and materials (such as corrosion, photoelectrochemistry, and battery materials) have yet to be examined in this way. The methods developed for discovering and optimizing electrocatalysts also hold significant promise for applications in these areas.

ACKNOWLEDGEMENTS

This work was supported by grants from the Army Research Office (grant DAAH04-94-G-0055) and by the Army Research Laboratory, Collaborative Technology Alliance in Power and Energy. We thank Drs Sasha Gorer and Peter Strasser for communicating the results in Refs. [60, 73] prior to publication.

REFERENCES

1. (a) A. Mittasch, *Adv. Catal.*, **2**, 81 (1950); (b) B. Timm, in '8th International Congress on Catalysis, Vol. 1, Plenary Lectures', Verlag Chemie, Weinheim, pp. 7–30 (1984).
2. J. J. Hanak, *J. Mater. Sci.*, **5**, 964 (1970).
3. (a) X.-D. Xiang, X. Sun, G. Briceno, Y. Lou, K.-A. Wang, H. Chang, W. G. Wallace-Friedman, S. Chen and P. G. Schultz, *Science*, **268**, 1738 (1995); (b) G. Briceno, H. Chang, X. Sun, P. G. Schultz and X.-D. Xiang, *Science*, **270**, 273 (1995).
4. (a) E. Danielson, J. H. Golden, E. W. McFarland, C. M. Reaves, W. H. Weinberg and X. D. Wu, *Nature (London)*, **389**, 944 (1997); (b) E. Danielson, M. Devenney, D. M. Giaquinta, J. H. Golden, R. C. Haushalter, E. W. McFarland, D. M. Poojary, C. M. Reaves, W. H. Weinberg and X. D. Wu, *Science*, **279**, 837 (1998).
5. R. B. van Dover, L. F. Schneemeyer and R. M. Fleming, *Nature (London)*, **392**, 162 (1998).
6. (a) T. A. Dickinson, D. R. Walt, J. White and J. S. Kauer, *Anal. Chem.*, **69**, 3413 (1997); (b) Y. P. Sun, H. Buck and T. E. Mallouk, *Anal. Chem.*, **73**, 1599 (2001).
7. B. M. Cole, K. D. Shimizu, C. A. Krueger, J. P. A. Harrity, M. L. Snapper and A. H. Hoveyda, *Angew. Chem., Int Ed. Engl.*, **35**, 1668 (1996).
8. (a) F. C. Moates, M. Somani, J. Annamalai, J. T. Richardson, D. Luss and R. C. Willson, *Ind. Eng. Chem. Res.*, **35**, 4801 (1996); (b) S. Senkan, *Nature (London)*, **394**, 350 (1998); (c) P. Cong, R. D. Doolen, Q. Fan, D. M. Giaquinta, S. Guan, E. W. McFarland, D. M. Poojary, K. Self, H. W. Turner and W. H. Weinberg, *Angew. Chem., Int Ed. Engl.*, **38**, 484 (1999); (d) A. M. Cassell, S. Verma, L. Delzeit, M. Meyyappan and J. Han, *Langmuir*, **17**, 260 (2001).
9. (a) A. Holzwarth, P. W. Schmidt and W. E. Maier, *Angew. Chem.*, **110**, 2788 (1998); (b) M. Orschel, J. Klein, H. W. Schmidt and W. F. Maier, *Angew. Chem.*, **111**, 2961 (1999); (c) S. Senkan and S. Ozturk, *Angew. Chem.*, **111**, 867 (1999); (d) S. Senkan, K. Krantz, S. Ozturk, V. Zengin and I. Onal, *Angew. Chem.*, **111**, 2965 (1999); (e) K. Krantz, S. Ozturk and S. Senkan, *Catal. Today*, **62**, 281 (2000).
10. D. E. Akporiaye, I. M. Dahl, A. Karlsson and R. Wendelbo, *Angew. Chem., Int Ed. Engl.*, **37**, 609 (1998); (b) J. Klein, C. W. Lehmann, H. W. Schmid and W. F. Maier, *Angew. Chem., Int Ed. Engl.*, **37**, 3369 (1998); (c) U. Rodemerck, P. Ignaszewski, M. Lucas, P. Clau and M. Baerns, *Chem. Ing. Tech.*, **71**, 872 (1999); (d) P. Cong, A. Dehestani, R. Doolen, D. M. Giaquinta, S. Guan, V. Markov, D. Poojary, K. Self, H. W. Turner and W. H. Weinberg, *Proc. Natl. Acad. Sci. USA*, **96**, 11 077 (1999).
11. (a) S. J. Taylor and J. P. Morken, *Science*, **280**, 267 (1998); (b) A. C. Cooper, L. H. McAlexander, D.-H. Lee, M. T. Torres and R. H. Crabtree, *J. Am. Chem. Soc.*, **120**, 9971 (1998); (c) R. F. Harris, A. J. Nation, G. T. Copeland and S. J. Miller, *J. Am. Chem. Soc.*, **122**, 11 270 (2000); (d) M. Müller, T. W. Mathers and A. P. Davis, *Angew. Chem., Int Ed. Engl.*, **40**, 3813 (2001).
12. (a) B. Jandeleit, D. J. Schaefer, T. S. Powers, H. W. Turner and W. H. Weinberg, *Angew. Chem., Int Ed. Engl.*, **38**, 2494 (1999); (b) S. Senkan, *Angew. Chem., Int. Ed. Engl.*, **40**, 312 (2001); (c) J. N. Cawse, *Acc. Chem. Res.*, **34**, 213 (2001).
13. (a) M. E. Davis, *AIChE J.*, **45**, 2270 (1999); (b) M. Boudart, *Catal. Lett.*, **65**, 1 (2000).
14. G.-Q. Lu and A. Wieckowski, *Curr. Opin. Colloid Interface Sci.*, **5**, 95 (2000).

15. J. O'M. Bockris and H. Wroblowa, *J. Electroanal. Chem.*, **7**, 428 (1964); H. Dahms and J. O'M. Bockris, *J. Electrochem. Soc.*, **111**, 728 (1964).
16. M. M. P. Janssen and J. Moolhuysen, *Electrochim. Acta*, **21**, 869 (1976).
17. R. R. Adzic, W. E. O'Grady and S. Srinivasan, *J. Electrochem. Soc.*, **128**, 1913 (1981).
18. (a) F. Kadirgan, B. Beden, J. Leger and C. Lamy, *J. Electroanal. Chem.*, **125**, 89 (1981); (b) C. Lamy, *Electrochim. Acta*, **29**, 1584 (1984).
19. (a) M. Watanabe, Y. Furuuchi and S. Motoo, *J. Electroanal. Chem.*, **191**, 367 (1985); (b) M. Shibata and S. Motoo, *J. Electroanal. Chem.*, **209**, 151 (1986); (c) M. Watanabe, M. Uchida and S. Motoo, *J. Electroanal. Chem.*, **229**, 395 (1987).
20. S. Szabo and I. Bakos, *J. Electroanal. Chem.*, **230**, 233 (1987).
21. (a) H. A. Gasteiger, N. Markovic, P. N. Ross, Jr and E. J. Cairnes, *J. Phys. Chem.*, **98**, 617 (1994); (b) N. M. Markovic, H. A. Gasteiger, P. N. Ross, X. Jiang, I. Villegas and M. J. Weaver, *Electrochim. Acta*, **40**, 91 (1995).
22. R. Parsons and T. Vandernoot, *J. Electroanal. Chem.*, **257**, 9 (1998).
23. T. Frelink, W. Vissher, A. P. Cox and J. A. R. van Veen, *Electrochim. Acta*, **40**, 1537 (1995).
24. K. A. Friedrich, K. P. Geyzers, U. Linke, U. Stimming and J. Stumper, *J. Electroanal. Chem.*, **402**, 123 (1996).
25. T. Iwasita, F. C. Nart and W. Vielstich, *Ber. Bunsen-Ges. Phys. Chem.*, **94**, 1030 (1990).
26. Y. Tong, H. S. Kim, P. K. Babu, P. Waszczuk, A. Wieckowski and E. Oldfield, *J. Am. Chem. Soc.*, **124**, 468 (2002).
27. (a) T. Frelink, W. Visscher and J. A. R. van Veen, *Surf. Sci.*, **335**, 353 (1995); (b) T. Frelink, W. Visscher and J. A. R. van Veen, *Langmuir*, **12**, 3702 (1996).
28. P. Waszczuk, A. Wieckowski, P. Zelenay, S. Gottesfeld, C. Coutanceau, J.-M. Leger and C. Lamy, *J. Electroanal. Chem.*, **511**, 55 (2001).
29. J. W. Long, R. M. Stroud, K. E. Swider-Lyons and D. R. Rolison, *J. Phys. Chem. B*, **104**, 9772 (2000).
30. A. S. Arico, Z. Poltarzewski, H. Kim, A. Morana, N. Giordano and V. Antonucci, *J. Power Sources*, **55**, 159 (1995).
31. K. L. Ley, R. Liu, C. Pu, Q. Fan, N. Leyarovska, C. Segre and E. S. Smotkin, *J. Electrochem. Soc.*, **144**, 1543 (1997).
32. S. Mukerjee, S. J. Lee, E. A. Ticianelli, J. McBreen, B. N. Grgur, N. M. Markovic, P. N. Ross, J. R. Giallombardo and E. S. De Castroc, *Electrochem. Solid-State Lett.*, **2**, 12 (1999).
33. M. Goetz and H. Wendt, *J. Appl. Electrochem.*, **31**, 811 (2001).
34. E. Reddington, J.-S. Yu, A. Sapienza, B. C. Chan, B. Gurau, R. Viswanathan, R. Liu, E. S. Smotkin, S. Sarangapani and T. E. Mallouk, 'Combinatorial Discovery of and Optimization of New Electrocatalysts', in "Combinatorial Chemistry: A Practical Approach", H. Fenniri (Ed), Oxford University Press, Oxford, pp. 401–420 (2000).
35. P. N. Rylander, L. Haybrouck, S. G. Hindin, R. Iverson, I. Karpenko and G. R. Pond, *Engelhard Ind. Tech. Bull.*, **8**, 93 (1967).
36. E. M. Crabb, R. Marshall and D. Thompsett, *J. Electrochem. Soc.*, **147**, 4440 (2000).
37. (a) H. Bönnemann, W. Brijoux, R. Brinkmann, E. Dinjus, T. Joussen and B. Korall, *Angew. Chem., Int Ed. Engl.*, **30**, 1312 (1991); (b) T. J. Schmidt, M. Noeske, H. A. Gasteiger, R. J. Behm, P. Britz, W. Brijoux and H. Bönnemann, *Langmuir*, **13**, 2591 (1997).
38. M. Watanabe, M. Uchida and S. Motoo, *J. Electroanal. Chem. Interfacial Electrochem.*, **229**, 395 (1987).
39. T. E. Mallouk, E. Reddington, C. Pu, K. L. Ley and E. S. Smotkin, 'Discovery of Methanol Electro-Oxidation Catalysts by Combinatorial Analysis', in "Fuel Cell Seminar Extended Abstracts", Orlando, FL, pp. 686–689 (1996).
40. E. Reddington, A. Sapienza, B. Gurau, R. Viswanathan, S. Sarangapani, E. S. Smotkin and T. E. Mallouk, *Science*, **280**, 1735 (1998).
41. E. Reddington, J.-S. Yu, A. Sapienza, B. C. Chan, B. Gurau, R. Viswanathan, R. Liu, E. S. Smotkin, S. Sarangapani and T. E. Mallouk, in 'Advanced Catalytic Materials', P. W. Lednor, D. A. Nakagi and L. T. Thompson (Eds), MRS Symposium Proceedings, Vol. 549, pp. 231–236 (1999).
42. G. Chen, D. A. Delafuente, S. Sarangapani and T. E. Mallouk, *Catal. Today*, **67**, 341 (2001); (b) G. Chen, S. R. Bare and T. E. Mallouk, *J. Electrochem. Soc.*, in press.
43. Y. Sun, H. Buck and T. E. Mallouk, *Anal. Chem.*, **73**, 1599 (2001).
44. N. D. Morris and T. E. Mallouk, *J. Am. Chem. Soc.*, in press.
45. (a) A. W. Czarnik, *Acc. Chem. Res.*, **27**, 302 (1994); (b) A. W. Czarnik, *Chem. Biol.*, **2**, 423 (1995).
46. D. W. McKee and F. J. Norton, *J. Catal.*, **3**, 252 (1964); D. W. McKee, *J. Catal.*, **14**, 355 (1969).
47. B. C. Chan, R. Ramnarayanan, R. Liu, R. Viswanathan, G. Chen, E. S. Smotkin and T. E. Mallouk, unpublished results.
48. M. G. Sullivan, H. Utomo, P. J. Fagan and M. D. Ward, *Anal. Chem.*, **71**, 4369 (1999).
49. C. J. Warren, R. C. Haushalter and L. Matsiev, US Patent, 6,187,164 (2001).
50. D. Chu and S. Gilman, *J. Electrochem. Soc.*, **143**, 1685 (1996).
51. R. Liu and E. S. Smotkin, *J. Electroanal. Chem.*, (2002) in press.
52. E. Gileadi, 'Electrode Kinetics for Chemists, Chemical Engineers and Materials Scientists', VCH Publishers, New York, p. 5 (1993).
53. (a) B. C. Shah and A. C. Hillier, *J. Electrochem. Soc.*, **147**, 3043 (2000); (b) K. Jambunathan, B. C. Shah, J. L. Hudson and A. C. Hillier, *J. Electroanal. Chem.*, **500**, 279 (2001); (c) S. Jayaraman and A. C. Hillier, *Langmuir*, **17**, 7857 (2001).
54. (a) A. J. Bard, F. R. F. Fan, J. Kwak and L. Ovadia, *Anal. Chem.*, **61**, 132 (1989); (b) A. J. Bard, F. R. F. Fan, D. T. Pierce, P. R. Unwin, D. O. Wipf and F. Zhou, *Science*, **254**, 68 (1991); (c) A. J. Bard, F. R. F. Fan and M. V. Mirkin, *Electroanal. Chem.*, **18**, 243 (1994); (d) A. J. Bard, F.-R. Fan and M. Mirkin, *Phys. Electrochem.*, 209 (1995).

55. A. R. Kucernak, P. B. Chowdhury, C. P. Wilde, G. H. Kelsall, Y. Y. Zhu and D. E. Williams, *Electrochim. Acta*, **45**, 4483 (2000).
56. A. Hamnett, *Catal. Today*, **38**, 445 (1997).
57. S. Gottesfeld and T. A. Zawodzinsky, *Adv. Electrochem. Sci. Eng.*, **5**, 291 (1997).
58. B. Gurau, R. Viswanathan, T. J. Lafrenz, R. Liu, K. L. Ley, E. S. Smotkin, E. Reddington, A. Sapienza, B. C. Chan, T. E. Mallouk and S. Sarangapani, *J. Phys. Chem. B*, **102**, 9997 (1998).
59. H. A. Gasteiger, N. Markovic, P. N. Ross and E. J. Cairns, *J. Electrochem. Soc.*, **141**, 1795 (1994).
60. (a) A. Gorer, World Pat. Appl., WO 00/54346 (2000); (b) P. Strasser, S. Gorer and M. Devenney, in 'International Symposium on Fuel Cells for Vehicles', O. Yamamoto (Ed), Electrochemical Society of Japan, Nagoya, p. 153 (2000).
61. D. Chu and S. Gilman, *J. Electrochem. Soc.*, **141**, 1770 (1994).
62. A. Kuver and K. Potje-Kamloth, *Electrochim. Acta*, **43**, 2527 (1998).
63. J. Cruickshank and K. Scott, *J. Power Sources*, **70**, 40 (1998).
64. (a) S. Mukerjee and S. Srinivasan, *J. Electroanal. Chem.*, **357**, 201 (1993); (b) S. Mukerjee, J. McBreen and S. Srinivasan, *Proc. Electrochem. Soc. (Oxygen Electrochemistry)*, **95-26**, 38 (1996).
65. T. Toda, H. Igarashi, H. Uchida and M. Watanabe, *J. Electrochem. Soc.*, **146**, 3750 (1999).
66. T. Itoh, US Patents, 4,794,054 (1988), 5,024,905 (1991) and 5,876,867 (1999).
67. S. Gamburzev, O. Velev, S. Srinivasan, A. Appleby, F. Lucaz and D. Wheeler, *Proc. Electrochem. Soc.*, **97-13**, 78 (1997).
68. N. Alonso-Vante and H. Tributsch, *Nature (London)*, **323**, 486 (1986).
69. N. Alonso-Vante, W. Jeagerman, H. Tributsch, W. Honle and K. Yvon, *J. Am. Chem. Soc.*, **109**, 3251 (1987).
70. (a) N. Alonso-Vante, M. Giersig and H. Tributsch, *J. Electrochem. Soc.*, **138**, 639 (1991); (b) N. Alonso-Vante, B. Schubert and H. Tributsch, *J. Catal.*, **112**, 384 (1988); (c) N. Alonso-Vante, B. Schubert and H. Tributsch, *Mater. Chem. Phys.*, **22**, 281 (1989); (d) N. Alonso-Vante, H. Tributsch and O. Solorza-Feria, *Electrochim. Acta*, **40**, 567 (1995).
71. R. Jiang and D. Chu, *J. Electrochem. Soc.*, **147**, 4605 (2000).
72. H. Tributsch, M. Bron, M. Hilgendorff, H. Schulenburg, I. Dorbandt, V. Eyert, P. Bodganoff and S. Fiechter, *J. Appl. Electrochem.*, **31**, 739 (2001).
73. P. Strasser, S. Gorer and M. Devenney, *Proc. Electrochem. Soc. (Direct Methanol Fuel Cells)*, **2001–4**, 191 (2001).
74. E. Yeager, *J. Mol. Catal.*, **38**, 5 (1986).
75. J.-S. Yu, A. Sapienza, E. Reddington, B. Y. Kim, B. C. Chan, G. Chen, R. E. Schaak, G. L. Egan, T. E. Mallouk, R. Liu and E. S. Smotkin, unpublished results.
76. (a) Y. B. Vassilyev, O. A. Khazova and N. N. Nikolaeva, *J. Electroanal. Chem.*, **196**, 105 (1985); (b) B. Beden, F. Largeaud, K. B. Kokoh and C. Lamy, *Electrochim. Acta*, **41**, 701 (1996); (c) I. T. Bae, E. Yeager, X. Xing and C. C. Liu, *J. Electroanal. Chem.*, **309**, 131 (1991).
77. (a) M. W. Hsiao, R. R. Adzic and E. B. Yeager, *J. Electrochem. Soc.*, **143**, 759 (1996); (b) R. R. Adzic, M. W. Hsiao and E. B. Yeager, *J. Electroanal. Chem.*, **260**, 475 (1989).
78. M. Sakamoto and K. Takamura, *Bioelectrochem. Bioenerg.*, **9**, 571 (1982).
79. (a) G. Kokkinidis and N. Xonoglou, *Bioelectrochem. Bioenerg.*, **14**, 375 (1985); (b) G. Wittstock, A. Strubing, R. Szargan and G. Werner, *J. Electroanal. Chem.*, **444**, 61 (1998).
80. L. Liu, C. Pu, R. Viswananthan, Q. Fan, R. Liu and E. S. Smotkin, *Electrochim. Acta*, **43**, 3657 (1998).
81. A. S. Arico, P. Creti, E. Modica, G. Monforte, V. Baglio and V. Antonucci, *Electrochim. Acta*, **45**, 4319 (2000).
82. H. N. Dinh, X. Ren, H. Garzon, P. Zelenay and S. Gottesfeld, *J. Electroanal. Chem.*, **491**, 222 (2000).
83. W. E. O'Grady, P. L. Hagans, K. I. Pandya and D. L. Maricle, *Langmuir*, **17**, 3047 (2001).
84. S. Maniguet, R. J. Mathew and A. E. Russell, *J. Phys. Chem. B*, **104**, 1998 (2000).
85. R. A. Lampitt, L. P. L. Carrette, M. P. Hogarth and A. E. Russell, *J. Electroanal. Chem.*, **460**, 80 (1999).
86. R. Viswanathan, G. Hou, R. Liu, S. R. Bare, F. Modica, G. Mickelson, C. U. Segre, N. Leyarovska and E. S. Smotkin, *J. Phys. Chem. B*, **106**, 3459 (2002).
87. J. A. Kerr, in 'CRC Handbook of Chemistry and Physics', 79th edition, D. R. Lide (Ed), CRC Press, Boca Raton, FL, Section 9–51 (1998).
88. R. Liu, H. Iddir, Q. Fan, G. Hou, A. Bo, K. L. Ley, E. S. Smotkin, Y.-E. Sung, H. Kim, S. Thomas and A. Wieckowski, *J. Phys. Chem. B*, **104**, 3518 (2000).
89. J. Kua and W. A. Goddard, III, *J. Am. Chem. Soc.*, **121**, 10 928 (1999).
90. H.-W. Lei, S. Suh, B. Gurau, B. Workie, R. Liu and E. S. Smotkin, *Electrochim. Acta*, **47**, 2913 (2002).